

Novel *MIP* gene mutation causes autosomal-dominant congenital cataract

Jing-Lan Ni¹, Hua-Ming Wen², Xiao-Sheng Huang³, Qian-Wen Li⁴, Jia-Min Cai³, Bao-Jian Fan⁵, Jun Zhao⁶

¹The Second Clinical Medical College, Jinan University, Shenzhen 518020, Guangdong Province, China

²Department of Ophthalmology, Dongguan Chang'an Hospital, Dongguan 523843, Guangdong Province, China

³Shenzhen Eye Hospital Affiliated to Jinan University, Shenzhen Eye Institute, Shenzhen 518040, Guangdong Province, China

⁴Department of Oral & Maxillofacial Surgery, Shenzhen Stomatology Hospital Affiliated to Shenzhen University, Shenzhen 518040, Guangdong Province, China

⁵Department of Neurosurgery, Massachusetts General Hospital and Harvard Medical School, Boston 02114, Massachusetts, USA

⁶Department of Ophthalmology, Shenzhen People's Hospital (the Second Clinical Medical College, Jinan University; the First Affiliated Hospital, Southern University of Science and Technology), Shenzhen 518020, Guangdong Province, China

Co-first authors: Jing-Lan Ni and Hua-Ming Wen

Correspondence to: Jun Zhao. Department of Ophthalmology, Shenzhen People's Hospital (the Second Clinical Medical College, Jinan University; the First Affiliated Hospital, Southern University of Science and Technology), Shenzhen 518020, Guangdong Province, China. doctorzhaojun@163.com; Hua-Ming Wen. Department of Ophthalmology, Dongguan Chang'an Hospital, Dongguan 523843, Guangdong Province, China. wenruxiang555@163.com

Received: 2023-10-20 Accepted: 2024-01-15

Abstract

• **AIM:** To identify disease-causative mutations in families with congenital cataract.

• **METHODS:** Two Chinese families with autosomal-dominant congenital cataract (ADCC) were recruited and underwent comprehensive eye examinations. Gene panel next-generation sequencing of common pathogenic genes of congenital cataract was performed in the proband of each family. Sanger sequencing was used to validate the candidate gene mutations and sequence the other family members for co-segregation analysis. The effect of sequence changes on protein structure and function was

predicted through bioinformatics analysis. Major intrinsic protein (MIP)-wildtype and MIP-G29R plasmids were constructed and microinjected into zebrafish single-cell stage embryos. Zebrafish embryonic lens phenotypes were screened using confocal microscopy.

• **RESULTS:** A novel heterozygous mutation (c.85G>A; p.G29R) in the *MIP* gene was identified in the proband of one family. A known heterozygous mutation (c.97C>T; p.R33C; rs864309693) in *MIP* was found in the proband of another family. *In-silico* prediction indicated that the novel mutation might affect the MIP protein function. Zebrafish embryonic lens was uniformly transparent in both wild-type PCS2+MIP and mutant PCS2+MIP.

• **CONCLUSION:** Two missense mutations in the *MIP* gene in Chinese cataract families are identified, and one of which is novel. These findings expand the genetic spectrum of *MIP* mutations associated with cataracts. The functional studies suggest that the novel *MIP* mutation might not be a gain-of-function but a loss-of-function mutation.

• **KEYWORDS:** congenital cataract; major intrinsic protein; missense mutation; zebrafish model

DOI:10.18240/ijo.2024.03.06

Citation: Ni JL, Wen HM, Huang XS, Li QW, Cai JM, Fan BJ, Zhao J. Novel *MIP* gene mutation causes autosomal-dominant congenital cataract. *Int J Ophthalmol* 2024;17(3):454-465

INTRODUCTION

Congenital cataracts are one of the major causes of visual impairment in children, leading to irreversible blindness in approximately 10% of children with cataracts worldwide^[1]. According to the latest statistical data, the global prevalence of congenital cataracts was 0.60%^[2]. Both genetic and environmental factors play an important role in the aetiologies of congenital cataracts, among which genetic factors account for approximately 1/3 of cases^[3-4]. New causative genes for congenital cataracts have been reported in recent years. To date, at least 100 independent genetic loci, including more than 40 genes in different chromosomes, have been associated with congenital cataracts. Among these genes, lens protein and

connexins genes account for approximately 50% and 25%, respectively^[5]. The five main types of pathogenic genes are as follows: 1) lens protein genes, including *CRYAA*, *CRYAB*, *CRYBA1*, *CRYBA2*, *CRYBA4*, *CRYBB1*, *CRYBB2*, *CRYBB3*, *CRYGC*, *CRYGD*, and *CYRGS*; 2) membrane protein genes, such as *GJA3*, *GJA8*, major intrinsic protein (*MIP*), *LIM2*, *MP19*, and *PIKFYVE*; 3) cytoskeletal protein genes, such as *BFSP1* and *BFSP2*; 4) growth and transcription factor genes, including *CHX10*, *FOXE3*, *HSF4*, *MAF*, *PAX6*, and *PITX3*; 5) metabolic-related protein genes and other genes, such as *EPHA2*, *FTL*, *GALK1*, *GCNT2*, *CHMP4B*, and *NHS*.

Clinically, the phenotype of congenital cataracts is characterized by diversity and complexity, and its clinical phenotype has obvious genetic heterogeneity^[6]. It is of scientific and practical significance to discover new genes that affect cataractogenesis and to explore the cytological basis and molecular mechanism of their pathogenesis. In previous studies, we identified a potential pathological variant (p.G1943E) in *PIKFYVE* through whole-exome sequencing of a Chinese family with congenital cataract^[7]. We demonstrated that the haploinsufficiency of *PIKFYVE*^{G1943E} causes congenital cataract by using a zebrafish model. The *MIP* gene, a member of the aquaporin family, is the most abundant junction membrane protein in lens fibre cells, accounting for more than 60% of the total membrane protein content in these cells^[8]. It plays a crucial role in enabling the rapid movement of water on the cell membrane and controlling cellular water content^[9]. To date, more than 30 mutations in *MIP* have been associated with genetic cataracts in humans (Table 1)^[10-38]. In this study, we identified one novel and one known *MIP* gene mutation as causative mutations in two congenital cataract families.

SUBJECTS AND METHODS

Ethical Approval The study was approved by the Ethics Committee of Shenzhen Eye Hospital and was conducted in accordance with the ethical standards as laid down in the 1964 Declaration of Helsinki and its later amendments (the ethical approval number: 2020122401). All participants agreed for their samples to be used in other ethically approved studies. Informed consent was obtained from all participants. Clinical data were anonymised for analysis.

Pedigrees and Patients Two Chinese families with autosomal-dominant congenital cataract (ADCC) were recruited. Eight affected and five unaffected individuals were included; the patients were from the mountains of Yingde, Guangdong Province and Shangrao, Jiangxi Province, respectively.

All patients underwent detailed medical history collection and comprehensive eye examination. Data on family history, disease history, pregnancy history, ocular history, Snellen visual acuity, and best-corrected visual acuity were collected. Slit-lamp and anterior segment examinations were performed.

Genomic DNA Extraction and Library Construction

Peripheral blood samples (4-5 mL) were collected in EDTA anticoagulant vacuum tubes and stored at -20°C. Genomic DNA was extracted using a QIAamp DNA blood mini kit (Qiagen). DNA concentration and quality was determined using a NanodropTM 2000 spectrophotometer (Thermo Fisher Scientific Co., Ltd., Boston, MA, USA).

A ultrasonic DNA oscillator broke the DNA into 180-280 bp fragments. The adaptors at each end were ligated, and end repair and phosphorylation were performed. Ligation products were purified using magnetic beads. After purification suitable fragments were amplified by polymerase chain reaction (PCR).

Gene Panel Next-generation Sequencing The gene fragments were hybridized to the probe (whole-exon P039-exome probes) and adsorbed by the beads through biotin and streptavidin-biotin. Subsequently, the nonspecific binding DNA fragments were washed, and the target genes were enriched.

Gene panel sequencing was conducted on a NextSeq 500 sequencing system (Illumina, San Diego, CA, USA) using bridge amplification and a Flowcell sequencing chip (Illumina, San Diego, CA, USA). NextSeq 500 performed intelligent cycle imaging, in which individual cycle reactions could be extended with only one correct complementary base; the base species were confirmed based on distinct fluorescent signals followed by multiple cycles to yield the complete nucleic acid sequence.

Bioinformatics Analysis Primary sequencing reads were aligned to the human reference genome (hg19) using Burrows-Wheeler Aligner software (Bwa:bwa-0.7.10;http://bio-bwa.sourceforge.net/) after filtering out low-quality reads and potential adaptor contamination sequences. The aligned reads were processed using the Genome Analysis Toolkit (GATK; https://www.broadinstitute.org/gatk/) through a standard information analysis pipeline (https://samtools.sourceforge.net/), which included the detection, annotation, and analysis of single nucleotide polymorphisms (SNPs) and the insertion and deletion mutations. The reference databases used were HapMap, dbSNP138, Exome Sequencing Project, and Exome Aggregation Consortium.

Validation of Candidate Gene Mutations by Sanger Sequencing

Candidate *MIP* mutations were validated and genotyped in the other family members by Sanger sequencing. The corresponding coding regions of these genes were amplified and sequenced. PCR primers were designed using Primer 3.0 online software (Applied Biosystems ABI, Foster City, CA, USA). Sequences of the forward primers were as follows: (Pedigree A) 5'-GTGACTGCAGGATTGACGTG-3', reverse of 5'-GACTGTCCACCCAGACAAGG-3'; (Pedigree B) 5'-GTGACTGCAGGATTGACGTG-3', reverse of 5'-TTCACCCCACTTCTCGTAG-3'.

Table 1 Summary of mutations in the major intrinsic protein gene associated with genetic cataracts^[10-38]

Nucleotide change	Amino acid change	Inheritance	Phenotype	Region	Reference
c.2T>C	p.M1?	AD	Cerulean	China	[10]
c.67T>A	p.T23N	AR	Unknown	Pakistan	[11]
c.97C>T	p.R33C	AD	Posterior polar & nuclear	China	[12]
c.319G>A	p.V107I	AD	Sutural (lamellar)	China	[13]
c.337C>T	p.R113X	AD	Sutural (lamellar)	China	[14]
c.338G>A	p.R113Q	AR	Nuclear	Australia	[15]
c.401A>G	p.E134G	AD	Lamellar	The United Kingdom	[16]
c.402G>T	p.E134D	AD	Polymorphic	China	[17]
c.413C>G	p.T138R	AD	Polymorphic	The United Kingdom	[16]
c.448G>C	p.D150H	AD	Cortical punctate	China	[18]
c.489dupC	p.V164fs*37	AD	Nuclear	China	[19]
c.490G>A	p.V164I	AD	Anterior polar & nuclear	Australia	[15]
c.494G>A	p.G165D	AD	Total & lamellar	South India	[20]
c.500delC	p.A169Pfs*15	AD	Nuclear	China	[21]
c.508dupC	p.L170fs*31	AD	Nuclear	China	[22]
c.530A>G	p.Y177C	AD	Total & nuclear	China	[23]
c.559C>T	p.R187C	AD	Nuclear	China	[24]
c.572C>G	p.P191R	AD	Total	China	[25]
c.597_598insGGGAACATTCCACT	p.N200Gfs*12	AD	Punctate & lamellar	Australia	[26]
c.605G>A	p.W202X	AD	Unknown	United States	[27]
c.606+1G>A	splicing	AD	Nuclear	China	[28]
c.607-1G>A	p.LHS	AD	Cortical punctate	China	[29]
c.612C>G	p.Y204X	AD	Unknown	China	[30]
c.634G>C	p.G212R	AD	Sutural (lamellar)	China	[31]
c.644G>D	p.G215D	AD	Punctate	China	[32]
c.655delT	p.Y219Tfs*40	AD	Cortical & punctate	China	[33]
c.657C>G	p.Y219X	AD	Posterior polar	China	[34]
c.682_683delAA	p.K228fs*230	AD	Cortical punctate	China	[35]
c.702G>A	p.R233K	AD	Polymorphic	China	[36]
c.3223delG	p.G213Vfs*46	AD	Nuclear & cortical & punctate & lamellar	United States	[37]
IVS3-1G>A	p.V203fs	AD	Snail-like	China	[38]

AD: Autosomal dominant; AR: Autosomal recessive.

Protein Structure and Function Prediction ProtParam (<http://expasy.org/tools/protpar-am.html>) was used to predict the protein physicochemical properties. ProtScale (<https://web.expasy.org/protscale/>) was used for the hydrophobic analysis of mutant proteins and PolyPhen-2 (Polymorphism Phenotyping v2; <http://genetics.bwh.harvard.edu/pph2/index.shtml>) was used to predict the effect of mutations on protein function. Online SWISS-MODEL (<https://beta.swissmodel.expasy.org/interactive>) and SWISS-PDB viewer (<https://spdbv.vital-it.ch/>) tools were used to analyse the tertiary structure of the novel mutant MIP.

Construction of PCS2-MIP and PCS2-MIP^{G29R} Plasmid The coding region of the human *MIP* was obtained by PCR amplification of cDNA derived from the reverse transcription of human lens capsule RNA. The following primers were used: BamHI-MIP-1f

ACTGGATCCACCATGTGGGAACTGCGATCA and EcoRI-MIP-837r ATGCGAATTCTACAGGGCCTGGGTGTTCA. PCR amplification was performed using two primers, MIP and universal primers with Phusion DNA polymerase. After the procedures of agarose gel electrophoresis and purification, the products and the PCS2+ plasmids were linearized by using BamHI and EcoRI respectively. These digested products were purified with the QIAquick PCR purification kit (28104, QIAGEN) and were ligated by T4 ligase. Then mixed 3 µL of the ligated products with 50 µL of the DH5α competent cells for the transformation progress. The FastPure Plasmid Mini Kit (DC201, Vazyme) was used to extract plasmid DNA, which were validated by agarose gel electrophoresis. *BamHI* and *EcoRI* were used to linearize the products and validated by agarose gel electrophoresis to prove the *MIP* fragment was inserted successfully. The sp6 primer (sequence:

ATTTAGGTGACACTATAGA) was used to sequence the PCS2-MIP plasmid to verify its construction.

The PCS2-MIP plasmid was used as the template to construct the PCS2-MIP^{G29R} plasmid by creating a point mutation from guanine to adenine on the primer. The primer sequences were used: MIPGA-f CTATGTCTTCTTTGGGCTGAGGTCTCACT and MIPGA-r CAGCCCAAAGAAGACATAGAAGAGG. Validation, purification, extraction and revalidation of the plasmids from the purified products followed the same steps above. Sequencing with the sp6 primers was performed to assure the guanine was replaced by the adenine at amino acid 29.

In Vitro Synthesis of MIP and MIP^{G29R} mRNA PCS2-MIP and PCS2-MIP^{G29R} plasmids were linearized by using NotI-HF and left overnight in a 37°C incubator. The digested products were purified with the QIAquick PCR purification kit (28104, QIAGEN) which were used as the template for *in vitro* transcription. *In vitro* transcription was completed by using the mMessage mMachine SP6 transcription kit (Ambion).

mRNA Microinjection into Zebrafish Embryos MIP mRNA and MIP^{G29R} mRNA were diluted to 100 ng/μL and 300 ng/μL concentrations after *in vitro* transcription before microinjecting into zebrafish single-cell stage embryos at the first cell stage of the zygote, respectively, in a microinjection volume of approximately 2 nL. Embryos were raised and collected until embryonic development up to 72h, after which zebrafish embryonic lens phenotypes were screened under confocal microscopy. Both zebrafish husbandry and animal experiments were completed at the Medical Center, Hong Kong University of Science and Technology, Peking University, Shenzhen, China.

RESULTS

Clinical Characteristics of the Patients Two three-generation Chinese families with a clear diagnosis of ADCC were recruited (11 individuals affected and 16 individuals unaffected; Figure 1, Table 2). All affected individuals had varying degrees of opacified cataracts, and 13 family members (8 affected and 5 unaffected) participated in this study. The phenotypes of opacified cataracts in these families contained multiple forms. In Pedigree A, nuclear opacification in III:7-9, central nuclear calcification and peripheral cortical opacity in II:6, central nuclear calcification absorption and peripheral cortical opacity in I:2 were observed. All patients in Pedigrees A also showed nystagmus and strabismus, with an intraocular lens in another eye. In Pedigree B, typical Y gap turbidity with the right eye and scattered turbidity with the left eye in II:3, scattered punctate opacification in I:2 and III:3 were observed. The proband of Pedigree A was a 26-year-old woman (II:6) whose vision had decreased since birth. She had undergone right-eye cataract extraction at the age of 10y. To obtain further information about the cataract phenotype and collect blood

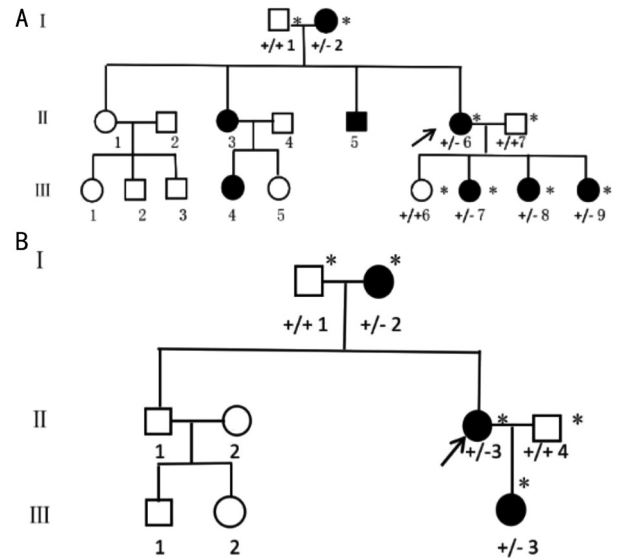


Figure 1 Pedigree of two Chinese families with ADCC Squares and circles indicate males and females, respectively. Black symbols indicate affected members and open symbols indicate unaffected individuals. The black arrow indicates the proband. Asterisks indicate family members who attended this study. Genotypes of the MIP mutation are indicated below each pedigree symbol (+, wild-type allele; -, mutant allele). ADCC: Autosomal-dominant congenital cataract.

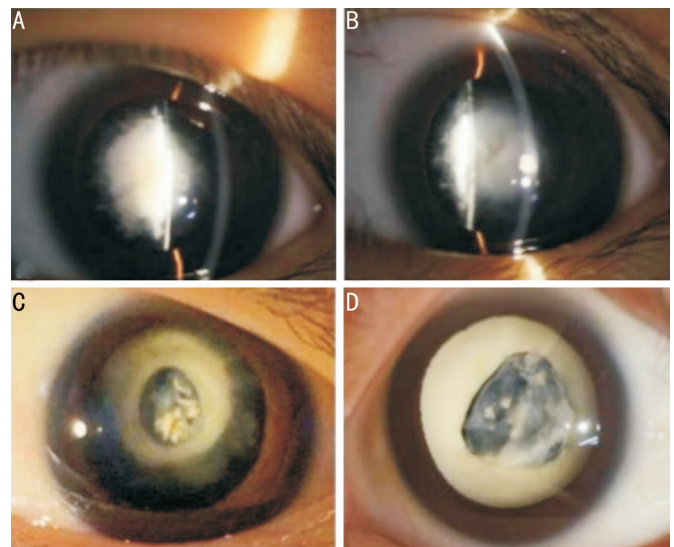


Figure 2 Phenotypic and clinical examination images of the affected members in Pedigree A A, B: Cataract phenotypes were nuclear opacification in juvenile members; C: Cataract phenotype in young member, with central nuclear calcification and peripheral cortical opacity; D: Cataract phenotype in elder member, with central nuclear calcification absorption and peripheral cortical opacity.

samples, we went to the family's residence and collected the cataract phenotypes of the five affected members. The pedigree phenotype varied among different age groups (Figure 2). The affected juvenile members (Figure 1A, III:7, 8, 9) aged from 3 to 9y, and the cataract phenotype was nuclear opacification (Figure 2A and 2B). The young member (Figure 1A, II:6) was 26 years old with central nuclear calcification and peripheral

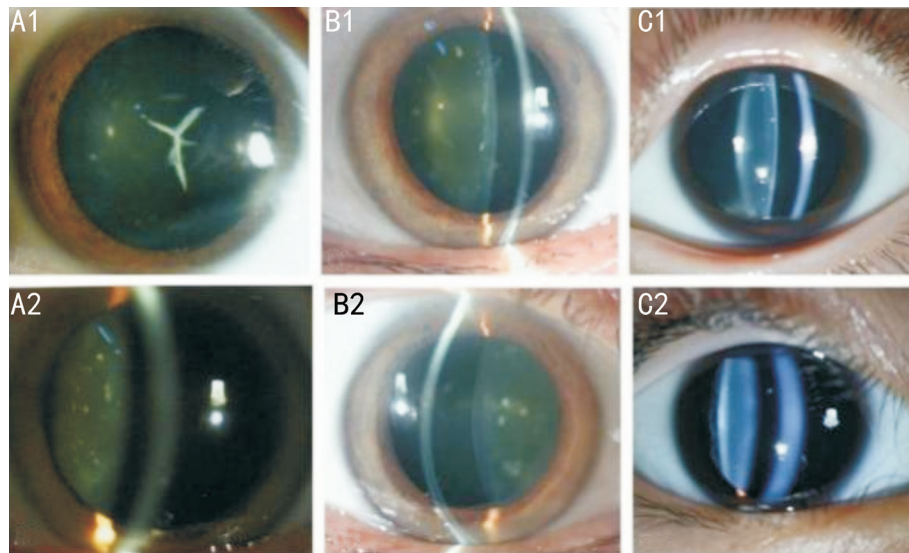


Figure 3 Phenotypic and clinical examination images of the affected members in Pedigree B A1, A2: The phenotypes of the left and right eyes of the proband were varying. The right eye had typical Y gap turbidity and the left eye had scattered turbidity. B1, B2: The mother of proband (I:2): cataract phenotypes were scattered punctate opacification; C1, C2: The daughter of proband (III:3): cataract phenotypes were scattered punctate opacification.

Table 2 Genotypes of the patients in Pedigrees A and B

Parameter	Pedigree A								Pedigree B				
	I:1	I:2	II:6	II:7	III:6	III:7	III:8	III:9	I:1	I:2	II:3	II:4	III:3
Genotypes	+/+	+/-	+/-	+/+	+/+	+/-	+/-	+/-	+/+	+/-	+/-	+/+	+/-
Gender	M	F	F	M	F	F	F	F	M	F	F	M	F
Age (y)	58	60	26	44	6	4	2	0.25	58	55	35	33	5

M: Male; F: Female.

cortical opacity (Figure 2C). The elderly patient (Figure 1A, I:2) was 60 years old, with central nuclear calcification absorption and peripheral cortical opacity (Figure 2D). The proband of the second family (Pedigree B) was a 35-year-old woman, and her mother and her daughter were also affected. Although they had no complaints of visual impact, the examination revealed cataracts. The daughter (B III:3) of the proband was invited to the hospital for examination and was found to have a congenital cataract phenotype (Figure 3). The different phenotypes of the left and right eyes of the proband were the most characteristic features of this family (Figure 3A1 and 3A2). The right eye had typical Y-gap turbidity and the left eye had scattered turbidity. The cataract phenotypes of mother (Figure 1B, I:2) and daughter (Figure 1B, III:3) of the proband showed scattered punctate opacification (Figure 3B1, 3B2, 3C1, 3C2). Both pedigree patients had no other ocular or systemic abnormalities or symptoms aside from cataracts.

Mutation Screening The gene panel sequencing comprised 188 lens genes. The pathogenic-related genes were >99% (10×), and the sequencing depth was 200(±30)×. A heterozygous mutation at position 85 of the *MIP* gene was identified in Pedigree B, c.85G>A (p.G29R), with the glycine 29 (Figure 4B) variant being arginine (Figure 4A). Given that the mutation was not found in public databases, including

the Human Gene Mutation Database, dbSNP Database, 1000 Genomes Project, Exome Sequencing Project, and genome aggregation database, it was considered a novel mutation. The mutation was evaluated as a suspected pathogenic variant according to the guidelines of the American College of Medical Genetics and Genomics. In addition, a known heterozygous mutation was identified in the *MIP* gene in Pedigree A, c.97C>T (p.R33C; rs864309693), and the amino acid 33 arginine variant was cysteine; this mutation has been reported in the literature^[31,39]. The sequence map of the wild-type *MIP* gene is available in the following websites: https://www.ncbi.nlm.nih.gov/nuccore/NM_012064.4?from=45&to=836&report=fasta and https://www.ncbi.nlm.nih.gov/protein/NP_036196.1?report=fasta.

MIP^{G29R} Protein Structure and Function Prediction The MIP^{G29R} mutant protein consisted of 263 amino acids and a molecular weight of 28220.89. The theoretical pI is 9.00. The instability index (II) was calculated as 36.45, and the stability classification of proteins was stable. ProtScale analysis showed that the mutant MIP (MIP^{G29R}) was more hydrophobic than the wild type (Figure 5). Bioinformatics analysis showed that the SIFT score, the PolyPhen-2 score, and the PROVEAN score of the MIP^{G29R} mutant was 0.000, 0.982, and -6.73, respectively. All three scores were consistent with a pathogenic mutant,

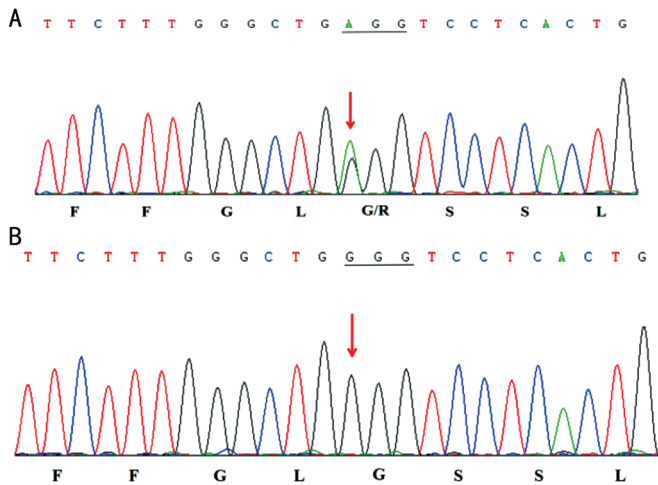


Figure 4 Pedigree A MIP gene mutation site with Sanger validation sequencing peak map A: DNA sequence chromatograms of the proband (II:3) showed a heterozygous c.85G>A nucleotide change in exon1 of MIP (red arrow) which altered the codon to AGG with the glycine 29 variant being arginine; B: DNA sequence chromatograms of an unaffected individual (I:1) showed GGG at the same codon (red arrow).

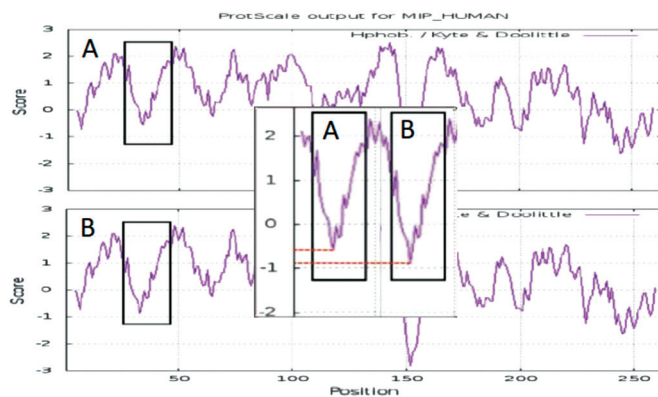


Figure 5 Predicting results of ProtScale ProtScale's prediction results showed that the MIP^{G29R} mutant had a higher hydrophobicity compared with the wild-type. A: The hydrophobicity of MIP^{G29R} mutant. B: The hydrophobicity of the B wild-type MIP. The substitution region on the MIP was boxed. Positive peak values indicate hydrophobic regions, and negative regions indicate hydrophilic regions. MIP: Major intrinsic protein.

indicating that the MIP protein was probably damaged, and the mutation might have affected protein function.

Self-Optimized Prediction Method from Alignment (SOPMA) was used to predict the secondary structures of the proteins. MIP^{G29R} protein: α -helix (38.78%), uncoiled (38.40%), β -fold (20.15%), and β -turn angle (2.66%). Wild-type MIP: α -helix (40.68%), coiled (37.26%), β -fold (20.16%), and β -angle (1.90%; Figure 6). It showed that the proportion of mutant protein α -helix decreased compared to the wild type, irregular coil increased, and no significant change was observed in β -fold and β -angle. We generated a 3D model of wild-type and MIP^{G29R} mutant proteins using the SWISS PDB viewer. The complex structures of MIP^{G29R} mutant proteins are shown in the

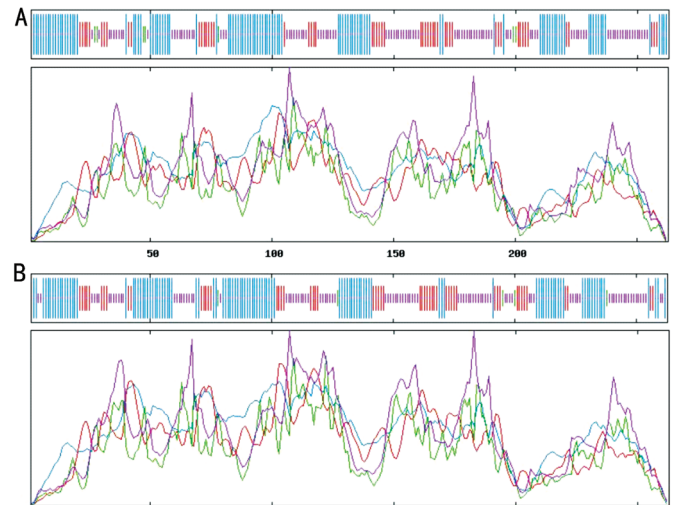


Figure 6 Prediction of secondary structures using Self-Optimized Prediction Method from Alignment (SOPMA) A: MIP^{G29R} protein: α -helix (38.78%) and uncoil (38.40%), β -fold (20.15%), and β -turn angle (2.66%). B: Wild-type MIP: α -helix (40.68%) and coiled (37.26%), β -fold (20.16%), and β -angle (1.90%). Blue: α -spiral; Purple: Uncurl; Red: β -fold; Green: β -corner.

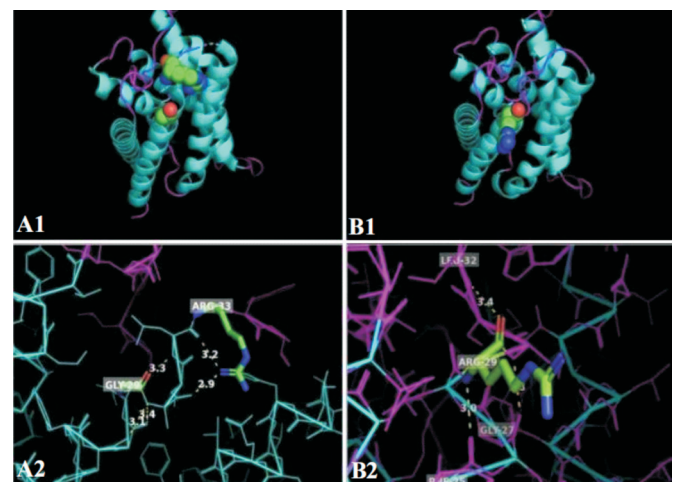


Figure 7 The 3D cartoon chart and hydrogen bond connection comparison chart The mutant may affect the stability of the protein structure region. The p.G29R mutant was found to perturb the amino acid chain and generate an extra hydrogen bond that interacted with p.F25, p.G27, and p.L32. The p.R33C mutant was found to perturb the amino acid chain and generate an extra hydrogen bonds that interacted with p.L32 and p.W34. A1, A2: Wild type MIP; B1, B2: MIP-p.G29R mutant.

cartoon chart and hydrogen bond connection comparison chart (Figure 7). The MIP^{G29R} sequence had 99.62% identity with wild-type MIP. This mutation could have affected the stability of the protein structure region. The MIP^{G29R} mutant disrupted the amino acid chain and generated additional hydrogen bonds that interacted with p.F25, p.G27, and p.L32.

Effects of Overexpression of Human MIP^{G29R} Mutant on Lens Development in Zebrafish PCR products and electrophoresis of the extracted plasmids showed that the two

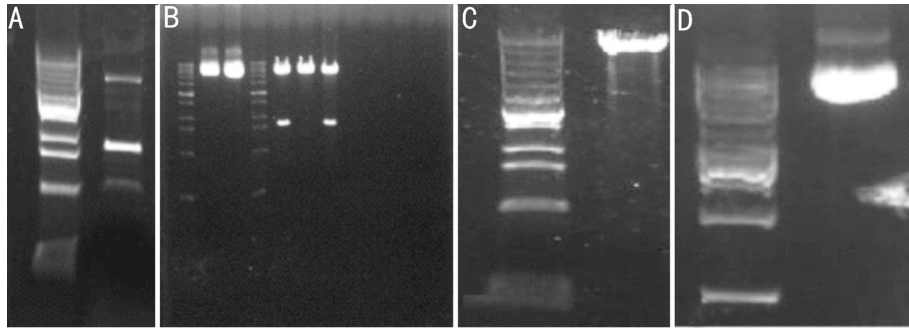


Figure 8 PCR products and electrophoresis of the extracted plasmids A: PCR products; B: PCS2+ and PCS2-MIP plasmid; C: PCR linear plasmid; D: PCS2-MIP^{G29R} plasmid. PCR: Polymerase chain reaction.

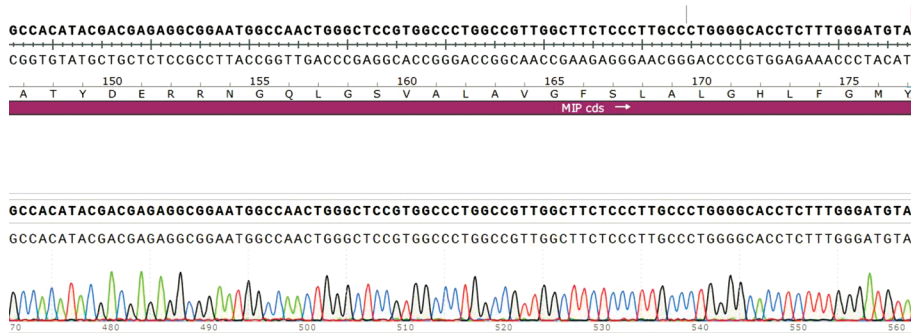


Figure 9 The sequencing results showed that the major intrinsic protein (*MIP*) gene sequence was identical to the *MIP* sequence in the database (only part of the *MIP* sequence is shown).

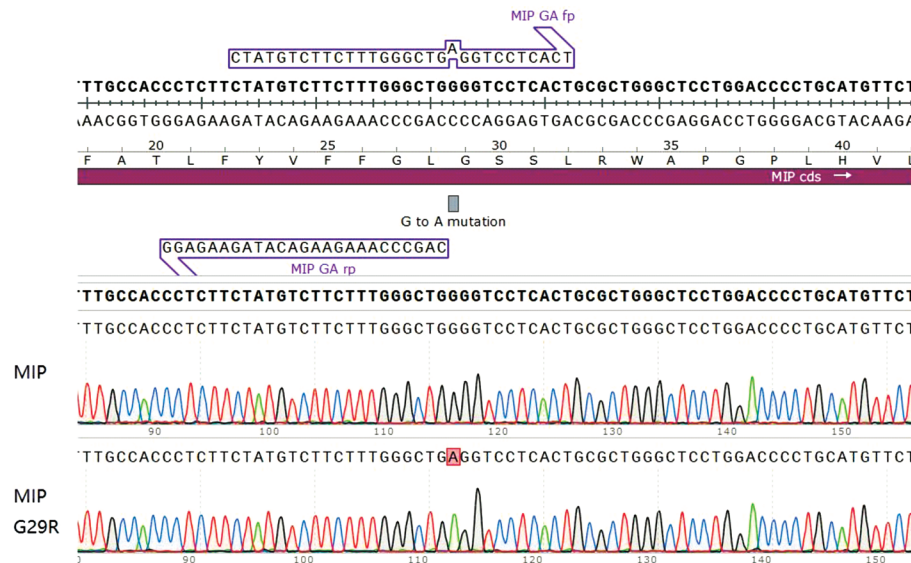


Figure 10 The PCS2-MIP plasmid was used to construct the PCS2-MIP^{G29R} plasmid. Sequencing of this plasmid with the sp6 primer showed that the guanine was replaced by the adenine at amino acid 29. The plasmid was constructed successfully.

plasmids could be cut into *MIP* fragments of 800 bp (Figure 8). This proved that *MIP* and *MIP*^{G29R} had been successfully inserted. The PCS2-MIP plasmid was sequenced with sp6 primers, and the sequencing results showed that the *MIP* sequence was identical to the *MIP* sequence in the database (Figure 9: only part of map is listed); therefore, the PCS2-MIP plasmid was successfully constructed.

The PCS2-MIP plasmid was used as the template to construct the PCS2-MIP^{G29R} plasmid by creating a point mutation from

guanine to adenine on the primer. Sequencing of the PCS2-MIP^{G29R} plasmid with the sp6 primer showed that the guanine was replaced by the adenine at amino acid 29 (Figure 10).

PCS2-MIP and PCS2-MIP^{G29R} plasmids were linearized by using NotI-HF. The digested products were purified and used as the template for *in vitro* transcription. The concentrations were determined by electrophoresis using the NanoDrop (Figure 11). The 100 ng/μL and 300 ng/μL concentrations of *MIP* mRNA and *MIP*^{G29R} mRNA were microinjected into

zebrafish embryos. The result showed that the microinjection of the 300 ng/ μ L concentration of mRNA were lethal to these embryos. The embryos microinjected with the 100 ng/ μ L concentration of mRNA were raised up to 72h, and the lens phenotypes were screened by confocal microscopy. We found that both wild-type and mutant PCS2+MIP lens fibres were uniformly transparent (Figure 12).

DISCUSSION

Aquaporins (AQPs) mainly mediate passive free water transfer across biofilms along the osmotic pressure gradient, thereby they play an important role in regulating lens water metabolism, maintaining lens internal microcirculation homeostasis, and participating in lens physiological functions and transparency^[40-41]. AQPs are a superfamily of MIPs of approximately 30 kDa that are expressed in prokaryotes and eukaryotes, three of which are present in the mammalian lens (AQP0, AQP1, and AQP5)^[42]. AQP0 is the most abundant AQP in the lens fibre cell membrane^[43], which is critical for lens transparency and homeostasis^[44]. It also performs a unique function of cell-to-cell adhesion between adjacent lens fibres regarding adhesion molecules, which is required for lens transparency^[45]. Originally known as MIP, AQP0 was later confirmed to belong to the aquaporin family. MIP promotes the movement of water into lens fibre cells, and in addition to serving as a water channel, it can act as an adhesion molecule squeezing highly ordered fibre cells and minimizing extracellular space and light scattering to maintain lens transparency^[46-47]. Bateman *et al*^[48] established *MIP* as a pathogenic gene in congenital cataracts in the year 2000. Several studies have shown that human and mouse *MIP* gene mutations can cause autosomal dominant cataracts. Any mutation in *MIP* may cause significant changes in protein folding that disrupt MIP transport mechanisms and water channel function, which directly affects the occurrence and development of the lens and leading to congenital cataracts. Conservation analysis showed that MIP was highly conserved in mammals. In this study, a novel heterozygous mutation (c.85G>A; p.G29R) in the *MIP* gene was identified in the proband of one family. A known heterozygous mutation (c.97C>T; p.R33C; rs864309693) in *MIP* was found in the proband of another family. These two mutations (p.R33C and p.G29R) are not located in functional domains and conserved sequence regions by UniProt database query; but they are located in the extracellular A loop and H1 area of the cell membrane, respectively.

The severity of congenital cataracts exhibits considerable heterogeneity and may be related to the significant influence of growth environment and development^[49]. Both congenital cataract families examined in this study had missense mutations in the *MIP* gene; however, significant differences were observed in the cataract phenotypes of the two families;

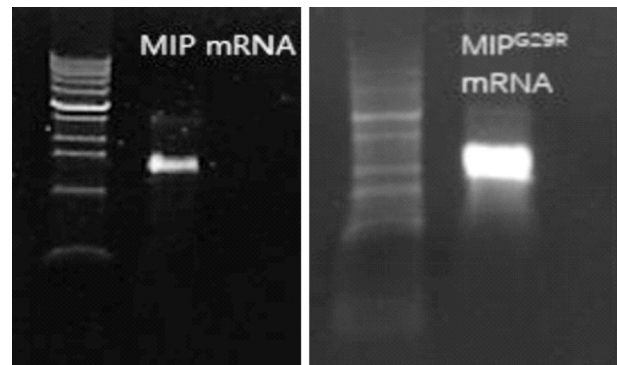


Figure 11 The PCS2-MIP and PCS2-MIP^{G29R} plasmids were linearized. MIP mRNA and MIP^{G29R} mRNA were transcribed *in vitro*.

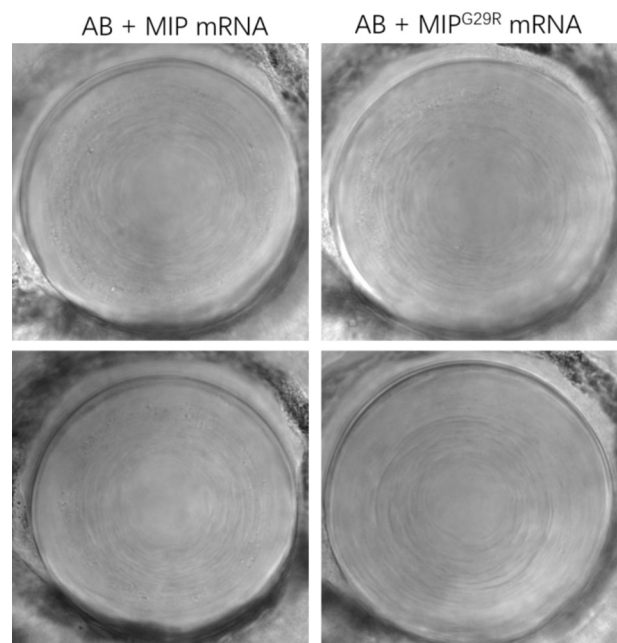


Figure 12 The embryos microinjected with the 100 ng/ μ L concentration of mRNA were raised until embryonic development up to 72h and then the lens phenotypes were screened by confocal microscopy. Lens fibers in both wild-type and mutant PCS2+MIP were uniformly transparent.

even within the same family, significant clinical heterogeneity was noted (Figures 2 and 3, Table 2). The mutation found in Pedigree A was consistent with the previously reported Chinese pedigree with ADCC^[12], where a missense mutation caused the change of arginine at amino acid 33 to cysteine (R33C), which significantly reduced the cell adhesion between the mutants. This mutation could affect the stability of the protein structure region. The mutation identified in Pedigree B has not been reported to date. Therefore, it was considered as a novel mutation. According to the American Society of Medical Genetics and Genomics guidelines, this variant may lead to loss of gene function with a low-frequency variant in the normal population database; the variant was judged as a suspected pathogenic variant.

ProtScale analysis revealed decreased hydrophobicity of MIP^{G29R} amino acids in the range of mutation regions

compared to the wild type. Hydrophobicity is conducive to the internal folding of the protein to form the α helix and further form the domain, which contribute to the stability of the tertiary structure^[50-52]. Thus, the reduced hydrophobicity of *MIP*^{G29R} amino acids in the range of mutated regions may be a factor affecting the protein domain function. In-silico analyses including SIFT, PolyPhen-2 and PROVEAN, indicate that might be a pathogenic mutation.

Secondary structure prediction of the *MIP*^{G29R} mutant showed that the hydrophobicity and the proportion of α -helices had been decreased (Figure 7), which may potentially affecting the protein folding process. These secondary structure changes may cause the formation of inconsistent domains, weaken their own stability, change the interaction between proteins and lead to lens opacity. The 3D models of wild-type and *MIP*^{G29R} mutant proteins suggest that the mutation site (p.G29R) was located in the H1 region of the cell membrane, affecting the stability of the protein structure. The *MIP*^{G29R} mutant may perturb the amino acid chains and produce additional hydrogen bonds that interact with p.F25, p.G27, and p.L32, leading to protein function changes. In terms of the nature of the affected amino acid, the glycine (G) side chain has only one hydrogen atom and does not contain any active group, while the arginine (R) side chain contains a guanidine group, which can form multiple hydrogen bonds, change the local charge distribution, bind to negatively charged molecules, and interact with the surrounding proteins. These results support a hypothesis of loss-of-function alterations that may affect aqua channel membrane protein function. Further *in vitro* experiments to elucidate the underlying pathogenic mechanisms and effects of the missense mutations observed in this family are warranted.

To further verify how this novel *MIP*^{G29R} mutation causes congenital cataract and whether it is a loss-of-function or a gain-of-function mutation, we constructed a human PCS2+*MIP*^{G29R} plasmid, which was microinjected into zebrafish embryos to observe lens development (Figure 12). Zebrafish is functionally similar to humans and is genetically highly conserved^[53-55]. The whole genome of zebrafish has been sequenced (<http://zebrafish.org/home/guide.php>), and its genome is approximately 87% homologous of the human genome^[56-57]. According to the Ensembl database (<http://www.ensembl.org/index.html>), the *MIP* gene is highly homologous and is expressed in its lens; therefore, zebrafish is a good model organism to study the pathogenesis of human cataracts caused by the *MIP* mutation.

The *MIP* missense mutation may cause congenital cataract in humans through two possible mechanisms. First, the mutated *MIP* is misfolded and cannot be transported from the endoplasmic reticulum, leading to the loss of function. Second, the mutation-formed heterozygotes exert a negative

effect, disrupting the balance of water in the lens, causing local precipitation of the lens. The mutated protein not only blocks the cell membrane channel but also affects other functional proteins. The novel *MIP* mutation in this study was located at position 85 of the H1 domain (c.85G>A) p.G29R, resulting in a missense change. To date, only one mutation in the H1 domain has been reported^[58], and there has been no study of protein function and animal experiments on the mutations in the H1 domain. In this study, zebrafish was used to verify whether the *MIP*^{G29R} missense mutation in the H1 domain causes congenital cataract *via* loss-of-function or gain-of-function. The results showed that crystal fibres in both wild-type and mutant PCS2-*MIP* were uniformly transparent, and no cataract phenotypes were observed in the zebrafish (Figure 12). Collectively, our results suggest a loss-of-function instead of a gain-of-function mechanism.

Many of the zebrafish orthologs currently identified are unclear as to whether they are true orthologs or have different explanations for the same gene. Due to the stochasticity and diversity of gene integration, the number of exogenous genes integrated within the zebrafish genome varies from locus to locus, resulting in progeny carrying the exogenous gene separation phenomenon^[59-60]. There are also questions regarding possible transgene silencing using promoter sequences from other species and the randomness of foreign gene integration sites. All these cases are likely to affect the expression of foreign genes and affect the experimental results. To provide further support on our loss-of-function hypothesis on this novel *MIP* mutation, we are planning to create a *MIP*^{G29R} mutant zebrafish strain using CRISPR/cas9 gene knockdown technology^[61-63].

In summary, we identified two missense mutations in *MIP* that cause ADCC in two Chinese families, one of which is a novel mutation. The novel mutation is located in the H1 domains of the *MIP* protein. Our zebrafish studies suggest that this novel *MIP*^{G29R} mutation is a loss-of-function mutation. Our findings expand the genetic spectrum of *MIP* mutations and validate the clinical and genetic heterogeneity of congenital cataracts.

ACKNOWLEDGEMENTS

Authors' contributions: Ni JL, Wen HM, Fan BJ, and Zhao J conceived and supervised the study. Wen HM, Zhao J, Huang XS, Cai JM, and Li QW recruited patients and Zhao J evaluated the patients' clinical manifestations. Ni JL, Zhao J, Wen HM, and Cai JM carried out mutation screening for candidate genes. Wen HM and Fan BJ performed data collection and analysis. Wen HM, Ni JL, Fan BJ, and Zhao J drafted and revised the manuscript.

Foundations: Supported by the Science, Technology and Innovation Commission of Shenzhen Municipality (No. GJHZ20220913142618036; No. JCYJ20210324113610029).

Conflicts of Interest: Ni JL, None; Wen HM, None; Huang XS, None; Li QW, None; Cai JM, None; Fan BJ, None; Zhao J, None.

REFERENCES

- 1 Tătaru CI, Tătaru CP, Costache A, Boruga O, Zemba M, Ciuluvică RC, Sima G. Congenital cataract - clinical and morphological aspects. *Rom J Morphol Embryol* 2020;61(1):105-112.
- 2 Yekta A, Hooshmand E, Saatchi M, Ostadimoghaddam H, Asharlous A, Taheri A, Khabazkhoob M. Global prevalence and causes of visual impairment and blindness in children: a systematic review and meta-analysis. *J Curr Ophthalmol* 2022;34(1):1-15.
- 3 Shiels A, Hejtmancik JF. Biology of inherited cataracts and opportunities for treatment. *Annu Rev Vis Sci* 2019;5:123-149.
- 4 Taylan Şekeroğlu H, Utine GE. Congenital cataract and its genetics: the era of next-generation sequencing. *Turk J Ophthalmol* 2021;51(2):107-113.
- 5 Shiels A, Hejtmancik JF. Inherited cataracts: genetic mechanisms and pathways new and old. *Exp Eye Res* 2021;209:108662.
- 6 Li JY, Chen XJ, Yan YB, Yao K. Molecular genetics of congenital cataracts. *Exp Eye Res* 2020;191:107872.
- 7 Mei SY, Wu Y, Wang Y, Cui YB, Zhang M, Zhang T, Huang XS, Yu SJ, Yu T, Zhao J. Disruption of PIKFYVE causes congenital cataract in human and zebrafish. *Elife* 2022;11:e71256.
- 8 Xu JW, Sun W, Du CX. Research progress in major intrinsic protein genes of congenital cataract. *Zhonghua Yan Ke Za Zhi* 2020;56(5):386-392.
- 9 Hall JE, Freitas JA, Tobias DJ. Experimental and simulation studies of aquaporin 0 water permeability and regulation. *Chem Rev* 2019;119(9):6015-6039.
- 10 Xiao XS, Li W, Wang PF, Li L, Li SQ, Jia XY, Sun WM, Guo XM, Zhang QJ. Cerulean cataract mapped to 12q13 and associated with a novel initiation codon mutation in MIP. *Mol Vis* 2011;17:2049-2055.
- 11 Chen JJ, Wang QW, Cabrera PE, Zhong ZL, Sun WM, Jiao XD, Chen YB, Govindarajan G, Naeem MA, Khan SN, Ali MH, Assir MZ, Rahman FU, Qazi ZA, Riazuddin S, Akram J, Riazuddin SA, Hejtmancik JF. Molecular genetic analysis of Pakistani families with autosomal recessive congenital cataracts by homozygosity screening. *Invest Ophthalmol Vis Sci* 2017;58(4):2207-2217.
- 12 Gu F, Zhai H, Li D, Zhao LX, Li C, Huang SZ, Ma X. A novel mutation in major intrinsic protein of the lens gene (MIP) underlies autosomal dominant cataract in a Chinese family. *Mol Vis* 2007;13:1651-1656.
- 13 Wang W, Jiang J, Zhu YN, Li JY, Jin CF, Shentu XC, Yao K. A novel mutation in the major intrinsic protein (MIP) associated with autosomal dominant congenital cataracts in a Chinese family. *Mol Vis* 2010;16:534-539.
- 14 Yu YB, Yu YH, Chen PQ, Li JY, Zhu YN, Zhai Y, Yao K. A novel MIP gene mutation associated with autosomal dominant congenital cataracts in a Chinese family. *BMC Med Genet* 2014;15:6.
- 15 Jones JL, McComish BJ, Staffieri SE, Souzeau E, Kearns LS, Elder JE, Charlesworth JC, MacKey DA, Ruddle JB, Taranath D, Pater J, Casey T, Craig JE, Burdon KP. Pathogenic genetic variants identified in Australian families with paediatric cataract. *BMJ Open Ophthalmol* 2022;7(1):e001064.
- 16 Berry V, Francis P, Kaushal S, Moore A, Bhattacharya S. Missense mutations in MIP underlie autosomal dominant 'polymorphic' and lamellar cataracts linked to 12q. *Nat Genet* 2000;25(1):15-17.
- 17 Liu S, Zhu P, Ni M, Zhang M, Jiang W, Yu M, Zhang J, Wu Q, Li W, Xue C, Xia X. A novel mutation of MIP in a Chinese family with congenital nuclear cataract identified by whole-exome sequencing. *Ophthalmic Genet* 2018;39(1):139-140.
- 18 Shentu XC, Miao Q, Tang XJ, Yin HF, Zhao YY. Identification and functional analysis of a novel MIP gene mutation associated with congenital cataract in a Chinese family. *PLoS One* 2015;10(5):e0126679.
- 19 Zhang XH, Wang JD, Jia HY, Zhang JS, Li Y, Xiong Y, Li J, Li XX, Huang Y, Zhu GY, Rong SS, Wormstone M, Wan XH. Mutation profiles of congenital cataract genes in 21 northern Chinese families. *Mol Vis* 2018;24:471-477.
- 20 Senthil Kumar G, Kyle JW, Minogue PJ, Dinesh Kumar K, Vasantha K, Berthoud VM, Beyer EC, Santhiya ST. An MIP/AQP0 mutation with impaired trafficking and function underlies an autosomal dominant congenital lamellar cataract. *Exp Eye Res* 2013;110:136-141.
- 21 Sun WM, Xiao XS, Li SQ, Guo XM, Zhang QJ. Exome sequencing of 18 Chinese families with congenital cataracts: a new sight of the NHS gene. *PLoS One* 2014;9(6):e100455.
- 22 Qin LT, Guo LJ, Wang HD, Li T, Lou GY, Guo QN, Hou QF, Liu HY, Liao SX, Liu Z. A novel MIP mutation in familial congenital nuclear cataracts. *Eur J Med Genet* 2016;59(9):488-491.
- 23 Yang GX, Zhang GS, Wu Q, Zhao JL. A novel mutation in the MIP gene is associated with autosomal dominant congenital nuclear cataract in a Chinese family. *Mol Vis* 2011;17:1320-1323.
- 24 Wang KJ, Li SS, Yun B, Ma WX, Jiang TG, Zhu SQ. A novel mutation in MIP associated with congenital nuclear cataract in a Chinese family. *Mol Vis* 2011;17:70-77.
- 25 Yuan C, Han TT, Su P, Liu M, Zhou XP, Zhang DZ, Jia WM, Wang AL, Yue M, Xiang ZB, Chen LM, Zhang XQ. A novel MIP mutation in a Chinese family with congenital cataract. *Ophthalmic Genet* 2018;39(4):473-476.
- 26 Ma AS, Grigg JR, Ho G, Prokudin I, Farnsworth E, Holman K, Cheng A, Billson FA, Martin F, Fraser C, Mowat D, Smith J, Christodoulou J, Flaherty M, Bennetts B, Jamieson RV. Sporadic and familial congenital cataracts: mutational spectrum and new diagnoses using next-generation sequencing. *Hum Mutat* 2016;37(4):371-384.
- 27 Reis LM, Tyler RC, Muheisen S, Raggio V, Salviati L, Han DP, Costakos D, Yonath H, Hall S, Power P, Semina EV. Whole exome sequencing in dominant cataract identifies a new causative factor, CRYBA2, and a variety of novel alleles in known genes. *Hum Genet* 2013;132(7):761-770.
- 28 Zeng L, Liu WQ, Feng WG, Wang X, Dang H, Gao LN, Yao J, Zhang XQ. A novel donor splice-site mutation of major intrinsic protein gene associated with congenital cataract in a Chinese family. *Mol Vis* 2013;19:2244-2249.

- 29 Jin CF, Jiang J, Wang W, Yao K. Identification of a MIP mutation that activates a cryptic acceptor splice site in the 3' untranslated region. *Mol Vis* 2010;16:2253-2258.
- 30 Li JY, Leng YJ, Han SR, Yan LL, Lu CX, Luo Y, Zhang X, Cao LH. Clinical and genetic characteristics of Chinese patients with familial or sporadic pediatric cataract. *Orphanet J Rare Dis* 2018;13(1):94.
- 31 Jiang B, Chen YH, Xu BS, Hong N, Liu RR, Qi M, Shen LP. Identification of a novel missense mutation of MIP in a Chinese family with congenital cataracts by target region capture sequencing. *Sci Rep* 2017;7:40129.
- 32 Ding XC, Zhou N, Lin H, Chen JJ, Zhao CY, Zhou GK, Hejtmancik JF, Qi YH. A novel MIP gene mutation analysis in a Chinese family affected with congenital progressive punctate cataract. *PLoS One* 2014;9(7):e102733.
- 33 Xiu Y, Fan Y, Wu K, Chen S, Pan M, Xu X, Zhu Y. A novel causative mutation for congenital cataract and its underlying pathogenesis. *Ophthalmic Genet* 2019;40(1):66-68.
- 34 Song ZX, Wang LQ, Liu YP, Xiao W. A novel nonsense mutation in the MIP gene linked to congenital posterior polar cataracts in a Chinese family. *PLoS One* 2015;10(3):e0119296.
- 35 Long XG, Huang YR, Tan H, Li Z, Zhang R, Linpeng SY, Lv WG, Cao YX, Li HX, Liang DS, Wu LQ. Identification of a novel MIP frameshift mutation associated with congenital cataract in a Chinese family by whole-exome sequencing and functional analysis. *Eye (Lond)* 2018;32(8):1359-1364.
- 36 Lin H, Hejtmancik JF, Qi YH. A substitution of arginine to lysine at the COOH-terminus of MIP caused a different binocular phenotype in a congenital cataract family. *Mol Vis* 2007;13:1822-1827.
- 37 Geyer DD, Spence MA, Johannes M, Flodman P, Clancy KP, Berry R, Sparkes RS, Jonsen MD, Isenberg SJ, Bateman JB. Novel single-base deletion mutation in major intrinsic protein (MIP) in autosomal dominant cataract. *Am J Ophthalmol* 2006;141(4):761-763.
- 38 Jiang J, Jin CF, Wang W, Tang XJ, Shentu XC, Wu RY, Wang Y, Xia K, Yao K. Identification of a novel splice-site mutation in MIP in a Chinese congenital cataract family. *Mol Vis* 2009;15:38-44.
- 39 Watanabe K, Wada KT, Ohashi T, Okubo S, Takekuma K, Hashizume R, Hayashi JI, Serikawa T, Kuramoto T, Kikkawa Y. A 5-bp insertion in Mip causes recessive congenital cataract in KFRS4/Kyo rats. *PLoS One* 2012;7(11):e50737.
- 40 Schey KL, Gletten RB, O'Neale CVT, Wang Z, Petrova RS, Donaldson PJ. Lens aquaporins in health and disease: location is everything!. *Front Physiol* 2022;13:882550.
- 41 Li Z, Quan YM, Gu SM, Jiang JX. Beyond the channels: adhesion functions of aquaporin 0 and connexin 50 in lens development. *Front Cell Dev Biol* 2022;10:866980.
- 42 Zhang KE, Di GH, Bai Y, Liu AX, Bian WH, Chen P. Aquaporin 5 in the eye: expression, function, and roles in ocular diseases. *Exp Eye Res* 2023;233:109557.
- 43 Freitas JA, Németh-Cahalan KL, Hall JE, Tobias DJ. Cooperativity and allosterism in aquaporin 0 regulation by Ca²⁺. *Biochim Biophys Acta Biomembr* 2019;1861(5):988-996.
- 44 Giannone AA, Li LP, Sellitto C, White TW. Physiological mechanisms regulating lens transport. *Front Physiol* 2021;12:818649.
- 45 Kumari S, Taginik G, Varadaraj S, Varadaraj K. Positively charged amino acid residues in the extracellular loops A and C of lens aquaporin 0 interact with the negative charges in the plasma membrane to facilitate cell-to-cell adhesion. *Exp Eye Res* 2019;185:107682.
- 46 Edamana S, Login FH, Yamada S, Kwon TH, Nejsum LN. Aquaporin water channels as regulators of cell-cell adhesion proteins. *Am J Physiol Cell Physiol* 2021;320(5):C771-C777.
- 47 Yu YH, Qiao Y, Ye Y, Luo CQ, Yao K. A novel single-base deletion mutation of MIP impairs protein distribution and cell-to-cell adhesion in autosomal dominant cataracts in a Chinese family. *Am J Med Genet A* 2023.
- 48 Bateman JB, Johannes M, Flodman P, Geyer DD, Clancy KP, Heinzmann C, Kojis T, Berry R, Sparkes RS, Spence MA. A new locus for autosomal dominant cataract on chromosome 12q13. *Invest Ophthalmol Vis Sci* 2000;41(9):2665-2670.
- 49 Bremond-Gignac D, Daruich A, Robert MP, Valleix S. Recent developments in the management of congenital cataract. *Ann Transl Med* 2020;8(22):1545.
- 50 Tang S, Li JS, Huang GX, Yan LJ. Predicting protein surface property with its surface hydrophobicity. *Protein Pept Lett* 2021;28(8):938-944.
- 51 Sinha I, Garde S, Cramer SM. Comparative analysis of protein surface hydrophobicity maps determined by sparse sampling INDUS and spatial aggregation propensity. *J Phys Chem B* 2023;127(48):10304-10314.
- 52 Lamiable A, Bitard-Feildel T, Rebehmed J, Quintus F, Schoentgen F, Mornon JP, Callebaut I. A topology-based investigation of protein interaction sites using Hydrophobic Cluster Analysis. *Biochimie* 2019;167:68-80.
- 53 Choe SK, Kim CH. Zebrafish: a powerful model for genetics and genomics. *Int J Mol Sci* 2023;24(9):8169.
- 54 Can HD, Chanumolu SK, Gonzalez-Muñoz E, Prukudom S, Otu HH, Cibelli JB. Comparative analysis of single-cell transcriptomics in human and Zebrafish oocytes. *BMC Genomics* 2020;21(1):471.
- 55 Jimenez Gonzalez A, Baranasic D, Müller F. Zebrafish regulatory genomic resources for disease modelling and regeneration. *Dis Model Mech* 2023;16(8):dmm050280.
- 56 Hills M, Falconer E, O'Neill K, Sanders AD, Howe K, Guryev V, Lansdorp PM. Construction of whole genomes from scaffolds using single cell strand-seq data. *Int J Mol Sci* 2021;22(7):3617.
- 57 Yang HB, Luan Y, Liu TT, et al. A map of cis-regulatory elements and 3D genome structures in zebrafish. *Nature* 2020;588(7837):337-343.
- 58 Sun W, Xu JW, Gu YS, Du CX. The relationship between major intrinsic protein genes and cataract. *Int Ophthalmol* 2021;41(1):375-387.
- 59 Lawrence C. Advances in zebrafish husbandry and management. *Methods Cell Biol* 2011;104:429-451.

- 60 Crim MJ, Lawrence C. A fish is not a mouse: understanding differences in background genetics is critical for reproducibility. *Lab Anim* 2021;50(1):19-25.
- 61 Hu XM, Zhang BB, Li XL, Li M, Wang YG, Dan HD, Zhou JM, Wei YM, Ge KK, Li P, Song ZM. The application and progression of CRISPR/Cas9 technology in ophthalmological diseases. *Eye (Lond)* 2023;37:607-617.
- 62 Jarayseh T, Guillemyn B, De Saffel H, *et al.* A *tapt1* knock-out zebrafish line with aberrant lens development and impaired vision models human early-onset cataract. *Hum Genet* 2023;142(3):457-476.
- 63 Zhao DR, Jones JL, Gasperini RJ, Charlesworth JC, Liu GS, Burdon KP. Rapid and efficient cataract gene evaluation in F0 zebrafish using CRISPR-Cas9 ribonucleoprotein complexes. *Methods* 2021;194:37-47.